Available online at www.sciencedirect.com
ScienceDirect
Icarus 195 (2008) 918–926
ICARUS
www.elsevier.com/locate/icarus

Bidirectional reflectance spectroscopy 6. Effects of porosity

Bruce Hapke

Department of Geology and Planetary Science, University of Pittsburgh, 200 SRCC Bldg., 4107 O'Hara St., Pittsburgh, PA 15260, USA

Received 13 June 2007; revised 19 November 2007

Available online 1 February 2008

Abstract

It is well known that the bidirectional reflectance of a particulate medium such as a planetary regolith depends on the porosity, in contrast to predictions of models based on the equation of radiative transfer as usually formulated. It is shown that this failure to predict porosity dependence arises from an incorrect treatment of the light that passes between the particles. In this paper a more physically correct treatment that takes account of the necessity of preventing particles from interpenetrating is used together with the two-stream approximation to solve the radiative transfer equation and derive improved expressions for the bidirectional and directional-hemispherical reflectances. It is found that increasing the filling factor (decreasing the porosity) increases the reflectance of low and medium albedo powders, but decreases it for ones with very high albedos. The model agrees qualitatively with measured data.

Keywords: Radiative transfer; Regoliths; Spectrophotometry

1. Introduction

It has been long known, but not widely appreciated, that the reflectance of a medium of particles larger than the wavelength depends on the porosity of the medium. Blevin and Brown (1961), Hapke and Wells (1981), Capaccioni et al. (1990), Kaasalainen (2003), Naranen et al. (2004) and Shepard and Helfenstein (2007) all found that the measured reflectances of powders in the laboratory increase as the as the porosity decreases. This is in contrast to the predictions of reflectance models based on the equation of radiative transfer (Hapke, 1981; Lumme and Bowell, 1981; Mishchenko et al., 1999) which, as usually formulated, is independent of porosity.

Interestingly, two other types of models do predict porosity dependence. The first uses Monte Carlo ray tracing methods. Peltoniemi and Lumme (1992) calculated the singly scattered reflectance of a medium of spheres and showed that the reflectance increased as the porosity decreased. They also pointed out that the multiply scattered contribution to the reflectance decreases at the same time because a medium of nonabsorbing particles must have a plane albedo (directional-hemispherical reflectance) equal to one, so that if the singly scattered radiation increases, the multiply scattered contribution must decrease.

The second type consists of models that consider the medium to be made of discrete layers of particles (Shkuratov et al., 1999; Hapke, 1999). This suggests a probable reason for the failure of models based on the radiative transfer equation, which assumes that the medium is continuous. In this paper the equation of radiative transfer is modified along the lines suggested by discrete layer models to make it quasi-continuous. These changes are then introduced into the reflectance model previously derived by the author (Hapke, 1981, 1993) and used to derive porosity-dependent expressions for the bidirectional reflectance and plane albedo.

This paper does not discuss the opposition effect, the surge in brightness at small phase angles. The reason is that the opposition effect is not intrinsically contained in the equation of radiative transfer, but must be added onto solutions of it in an *ad hoc* manner which is beyond the scope of this paper. The purpose of this paper is to show how porosity dependence can be introduced into the radiative transfer equation and expressions derived from it. Hence, this model is only valid outside of the opposition effect.

E-mail address: hapke@pitt.edu.

0019-1035/$ – see front matter
doi:10.1016/j.icarus.2008.01.003

2. Derivation

Consider a medium made of particles that vary in different ways, denoted by subscript i, such as size, shape, composition and crystalline structure. All particles are assumed to be large compared with the wavelength λ of light, equant, and randomly positioned and oriented. Let n_i denote the number of particles of type i per unit volume. Let v_i denote their volumes, σ_i their geometric cross sectional areas averaged over all orientations, and Q_{Si}, Q_{Ai}, and $Q_{Ei} = Q_{Si} + Q_{Ai}$ their scattering, absorption and extinction efficiencies, respectively. In this paper Q_{Si} only includes light intercepted by the physical cross-section of the particle, and does not include diffracted light, which will be treated separately. It will be assumed that the particles are sufficiently far apart that coherent effects can be neglected, so that to a good approximation Q_{Si} and Q_{Ai} are the same as when the particles are isolated. Let $p_i(g)$ be the phase function of the ith type of particle, where g is the phase angle. Initially it will be assumed that the particles scatter light isotropically so that $p_i(g) = 1$, although this requirement will be relaxed later. The medium fills the half-space $z < 0$, where the z axis is perpendicular to the surface. The surface is illuminated by collimated light of irradiance J making an angle i with the z axis, and is observed by a distant detector at an angle of viewing e and phase angle g.

It is assumed that the individual particles are the primary scatterers of the medium. Define the following:

total number of particles per unit volume,

$$n = \sum_i n_i; \tag{1}$$

filling factor (fraction of the volume occupied by solid particles),

$$\phi = \sum_i n_i v_i; \tag{2}$$

porosity,

$$P = 1 - \phi; \tag{3}$$

mean distance between particles (center-to-center),

$$L = n^{-1/3} \tag{4}$$

(L is also the mean thickness of a monolayer of particles);
scattering, absorption and extinction coefficients of the medium, respectively,

$$S = \sum_i n_i \sigma_i Q_{Si}, \qquad A = \sum_i n_i \sigma_i Q_{Ai},$$
$$E = \sum_i n_i \sigma_i Q_{Ei} = S + A; \tag{5}$$

single scattering albedo of the medium,

$$w = S/E; \tag{6}$$

mean particle volume,

$$v = \left(\sum_i n_i v_i\right) \Big/ \left(\sum_i n_i\right) = \phi/n; \tag{7}$$

mean particle geometric cross sectional area,

$$\sigma = \left(\sum_i n_i \sigma_i\right) \Big/ n; \tag{8}$$

mean scattering, absorption and extinction efficiencies, respectively,

$$Q_S = S/N\sigma, \qquad Q_A = A/N\sigma, \qquad Q_E = E/N\sigma; \tag{9}$$

mean particle phase function,

$$p(g) = \left[\sum_i n_i \sigma_i Q_{Si} p_i(g)\right] \Big/ S; \tag{10}$$

equivalent volume diameter,

$$D_v = \left(\frac{6}{\pi} v\right)^{1/3}; \tag{11}$$

equivalent area diameter,

$$D_\sigma = \left(\frac{4}{\pi}\sigma\right)^{1/2}; \tag{12}$$

D_v and D_σ are, respectively, the diameter of a sphere with the same volume and cross-sectional area as the average particle; if the particles are equant $D_v = D_\sigma \equiv D$. If the distribution of properties is continuous, the summations are replaced by integrals in these definitions.

Before proceeding with the derivation the question of why diffraction is excluded from Q_S, Q_E and $p(g)$ will be discussed. In order to calculate the multiply scattered contribution to the reflectance of a medium the quantities of interest are the intensity and lateral distribution of the radiance a few times L downstream from a monolayer generated by the portions of the wave that have passed between the particles in that monolayer. If the problem of the interaction of a plane electromagnetic wave with a sphere large compared to the wavelength is solved exactly using Maxwell's equations, one finds that the nature of the energy pattern around the sphere depends on the distance. Close to the sphere there is not only a wave propagating radially outward whose intensity falls off with the square of the distance, but also complicated patterns of near-fields and evanescent waves that extend of the order of a wavelength from the surface. Directly behind the sphere there is a shadow region. The edges of the shadow are not sharp, but have a ripple structure that may be thought of as if it were caused by waves generated by the edges of the particle interfering with the incident light that is passing by the sphere. The shadow and associated ripple structure are known as a Fresnel diffraction pattern.

As the distance to the particle increases the ripples spread out and fill in the shadow, until when $L \gg D \gg \lambda$ the shadow turns into a bright spot surrounded by faint rings, known as a Fraunhoffer diffraction pattern. The power in this pattern is equal to that intercepted by σ, and therefore it is common to define a diffraction efficiency $Q_{S\,\mathrm{diffraction}} = 1$ and treat it as if it were part of Q_S. For an isolated particle this pattern is then described as if it were light scattered by the particle, and Q_E taken to be approximately equal to 2.

However, the diffraction pattern is actually caused by portions of the incident light that have passed by the particle interfering constructively with each other and is not an intrinsic property of the particle. If the particle is in a powder or regolith it is closely surrounded by other particles. This alters the lateral distribution of the passing radiant power, which changes the diffraction pattern both quantitatively and qualitatively, decreasing it in intensity and causing it to become so narrow that it is indistinguishable from the collimated incident light (Hapke, 1999). The important thing to note is that conventional Fraunhoffer diffraction patterns do not exist within a particulate medium.

In media in which $L \sim D$ the patterns of light falling on particles behind other particles clearly are Fresnel diffraction patterns, not Fraunhoffer. Currently exact calculation of multiple scattering between particles can only be carried out by computer modeling of systems consisting of very small numbers of particles (Mishchenko et al., 2007; Petrova et al., 2007). Exact modeling of a regolith is hopelessly beyond current capabilities, so that approximate methods must be used. In order to obtain approximate expressions for the reflectance it will be assumed that the particles are randomly positioned and sample bright and shadowed regions in proportion to the relative areas of these regions. In this approximation the intensity pattern of light passing between the particles is assumed to be unscattered and is averaged laterally so that it is uniform with an intensity proportional to the fraction of open areas between particles. Then $Q_{\mathrm{S\,diffraction}} = 0$, $Q_{\mathrm{E}} \approx 1$, and $p(g)$ does not include a strong forward scattered Fraunhoffer diffraction peak.

The change in the radiance $I(z, \Omega)$ propagating through the medium at a depth z in a direction Ω making an angle θ with the z axis as it propagates through a monolayer of particles of thickness $\Delta s = L$ perpendicular to Ω is given by the equation of radiative transfer,

$$\Delta I(z, \Omega) = -EL I(z, \Omega) + \frac{SL}{4\pi} \int_{4\pi} I(z, \Omega')\, \mathrm{d}\Omega' + J \frac{SL}{4\pi} T(z/\mu_0). \tag{13}$$

The first term on the right describes the decrease in $I(z, \Omega)$ caused by absorption and scattering by particles within the layer; the second describes the increase due to scattering of radiance traveling in direction Ω' into direction Ω; and the third term is the source term of $I(z, \Omega)$ and describes the radiance of that fraction $T(z/\mu_0)$ of the incident irradiance J that has passed between the particles and penetrated to depth z where it is scattered by particles there; $T(z/\mu_0)$ is the transmissivity of the medium for the incident light.

In the usual formulation of the radiative transfer equation the medium is treated as if it were continuous. In that case the transmissivity, the fraction of radiation that is neither scattered nor absorbed, for light that has traveled a distance s through the medium is

$$T(s) = \exp(-Es). \tag{14}$$

However, that this is incorrect for a particulate medium can be seen as follows. The medium may be considered as being made up of a lattice of imaginary cubes with edges of length L, each containing the center of a particle somewhere inside it. In order that the particles do not overlap, each cube can contain only one particle. Consider a series of waves of radiance $I(z, \Omega)$ propagating through a particulate medium as they pass through a portion of a slab with area $A \gg L^2$ and thickness L oriented perpendicularly to the direction of travel. The slab contains nAL particles that, by the definition of a monolayer, do not shield one another from I. The amount of light that encounters particles in A and is extinguished (either scattered or absorbed) is $A\Delta I_{\mathrm{E}} = AILn\sigma Q_{\mathrm{E}} = AIEL$. The amount that passes between the particles is $A\Delta I_{\mathrm{T}} = AI - A\Delta I_{\mathrm{E}} = AI(1 - EL)$. Hence, the fraction of incident radiance transmitted by a monolayer of the medium is $\Delta I_{\mathrm{T}}/I = 1 - EL$.

Since the particles are assumed to be randomly positioned, the probability of transmission through several layers is the product of the probability in each layer. Thus, the fraction of light remaining after traversing a distance s consisting of $N = s/L$ layers is

$$T(s) = (1 - EL)^N = \exp\big[N \ln(1 - EL)\big] = \exp(-KEs), \tag{15}$$

where

$$K = -\ln(1 - EL)/EL. \tag{16}$$

Equation (15) is illustrated in Fig. 1, where $T(s)$ is seen to be a discontinuous stair function. The physical meaning of $T(s)$ is that the radiance on a particle located anywhere between $s = NL$ and $s = (N+1)L$ is $I_0(1-EL)^N$, where I_0 is the radiance incident on the first layer.

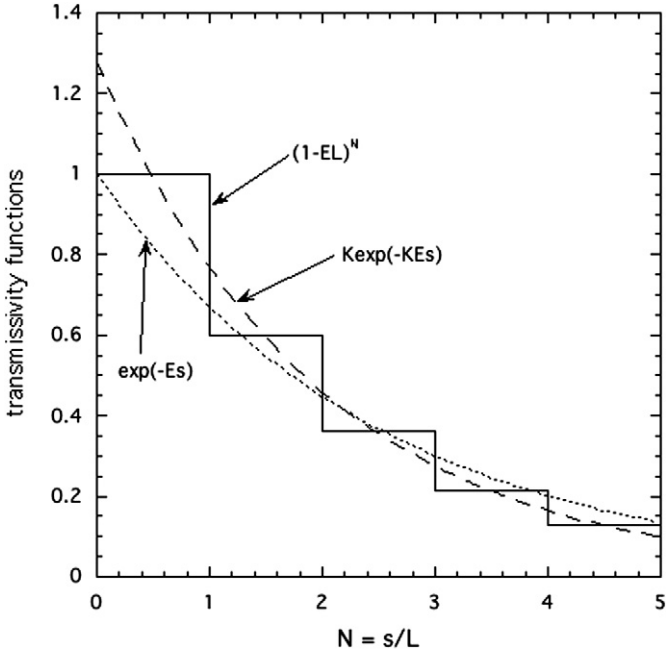

Fig. 1. Transmissivities vs number of the layer $N = s/L$ for the case $EL = 0.4$. The discontinuous stair function, Eq. (15) is plotted as the solid line and its continuous approximation, Eq. (26), as the dashed line. For comparison the transmissivity of a continuous medium, Eq. (14) is also shown.

Expanding K in a Taylor series

$$K = 1 + \frac{1}{2}EL + \frac{1}{3}(EL)^2 + \cdots \tag{17}$$

shows that $K > 1$. Hence, the unextinguished radiance falls off faster in a particulate medium than in a continuous medium with the same value of E and approximates propagation in a continuous medium only when the medium is so sparse that $EL \ll 1$. Fig. 1 also plots the transmission for a continuous medium, Eq. (14). Note that although the transmissivity falls off more rapidly in a particulate medium, the upper regions in a particulate medium actually receive more irradiance than in the continuous medium.

Now

$$\begin{aligned} EL &= n\sigma Q_E L = n^{2/3}\sigma Q_E = (\phi/v)^{2/3}\sigma Q_E \\ &= \frac{\pi D_\sigma^2/4}{(\pi D_v^3/6)^{2/3}}\phi^{2/3}Q_E \\ &= \left(\frac{3\sqrt{\pi}}{4}\right)^{2/3}\left(\frac{D_\sigma}{D_v}\right)^{2/3}Q_E\phi^{2/3} \\ &= 1.209\left(\frac{D_\sigma}{D_v}\right)^{2/3}Q_E\phi^{2/3}. \end{aligned} \tag{18}$$

We have seen that particles large compared to the wavelength have $Q_E \approx 1$ in a particulate medium, and if the particles are equant, $D_v \approx D_\sigma$; hence

$$EL \approx 1.209\phi^{2/3} = 1.209(1-P)^{2/3}. \tag{19}$$

The medium becomes opaque to directly transmitted light when $EL = 1$, or $\phi = 1.209^{-3/2} = 0.752$, or $P = 0.248$. This critical value of ϕ may be derived in a different way. When the medium just becomes opaque, the cross-sectional area of each cube is statistically just blocked by the cross-sectional area of the average particle, or $L^2 = \sigma = (\pi/4)D^2$, so $\phi = (\pi/6)D^3/L^3 = (\pi/6)(4/\pi)^{3/2} = 0.752$.

A numerical result equivalent to (15) can also be obtained from statistical mechanics considerations by computer calculation of the structure factor using the Percus–Yevic pair-correlation approximation (Mishchenko and Macke, 1997), provided that the particles are perfect spheres all of the same size. The structure factor essentially ensures that the particles do not overlap. The factor K performs the same role, but Eq. (15) is much more general and applies to particles of arbitrary shapes and size distribution (Hapke, 1999). It also has the advantage of being analytic. Equation (15) shows that for large particles the effective extinction coefficient in the transmissivity in a particulate medium is KE, rather than E. Ishimaru and Kuga (1982) observed an increase consistent with this in transmission measurements of thin layers of particles. Hapke (1986, 1993) derived a similar result, except that his equation for K equivalent to (16) was given by $-\ln(1-\phi)/\phi$. This result is now seen to be only approximately correct.

Before the limiting filling factor $\phi = 0.752$ is reached coherent interactions between particles become important. Such interactions are expected when not only the amplitudes but also the phase differences between the waves scattered by the particles must be taken into account. Other effects, such as particles interacting with the near-fields and evanescent waves of adjacent particles also become important. These all occur when the medium is so closely packed that the particles are separated by less than a wavelength; that is, when

$$L - D < \lambda. \tag{20}$$

Dividing by D, rearranging and cubing gives

$$\left(\frac{L}{D}\right)^3 = \frac{1}{nD^3} = \frac{v}{\phi D^3} < \left(1 + \frac{\lambda}{D}\right)^3, \tag{21}$$

or

$$\phi > \frac{v/D^3}{(1+\lambda/D)^3}. \tag{22}$$

For a medium of equant particles $v \approx (\pi/6)D^3$ and (22) is

$$\phi > \frac{\pi/6}{(1+\lambda/D)^3} = \frac{0.524}{(1+\lambda/D)^3}. \tag{23}$$

Equation (23) is plotted in Fig. 2 and shows that coherent effects must be taken into account in a medium of large particles when $\phi > \sim 50\%$. When this critical value of the filling factor is exceeded chains and clusters of smaller particles begin to scatter light as if they were single larger particles. The area in Fig. 2 between Eq. (23) and $\phi = 1$ marks the transition region where the propagation properties change from those of a nearly-continuous void containing some solid particles to a nearly-continuous solid containing some voids. In this region the amount of scattering per particle decreases (Gobel et al., 1995) and the particle phase functions become more forward scattering, causing the reflectance to decrease, as observed by Blevin and Brown (1961). When this occurs the model of this paper is no longer applicable. This paper is concerned with the region below Eq. (23).

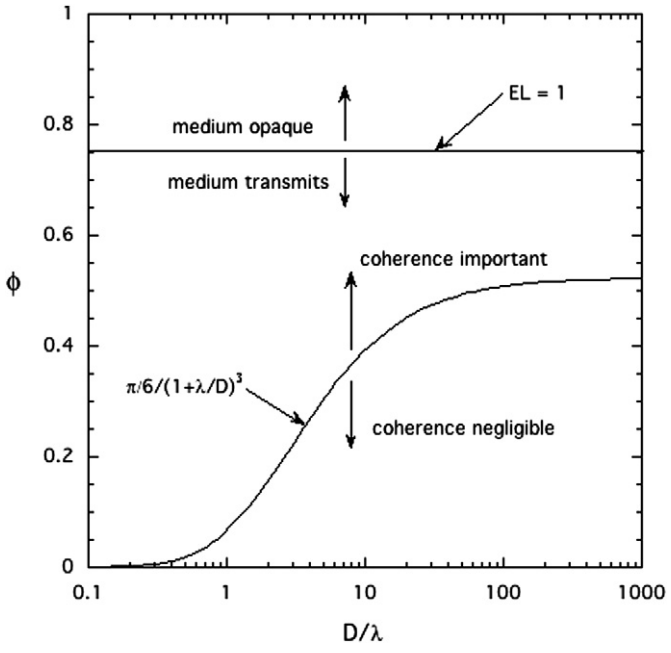

Fig. 2. Critical filling factors vs D/λ, showing the regions where coherent interference effects are important and where the medium becomes opaque to directly transmitted radiation.

The value of ϕ in a particulate medium depends critically on the size distribution. Most powders in the laboratory have $\sim 0.1 < \phi < \sim 0.5$. Very fine powders are cohesive and can have small filling factors (e.g., powdered sugar), while coarse powders tend to have larger ϕ (e.g., granular sugar). In powders with a wide size distribution smaller particles can fill in the spaces between big ones so that ϕ can approach 1. (This principle was used by the ancient Greeks in the construction of their walls without mortar.) Unfortunately, there are no *in situ* measurements of planetary regoliths. Based on a variety of indirect estimates (Heiken et al., 1991) the filling factor of lunar regolith appears to be relatively low (~0.3) at the surface, but increases extremely rapidly with depth to as much as ~0.9 at a depth of a few centimeters.

Equations (13) and (15) describe a medium of discrete layers. In order to make the model analytically tractable it is desirable to approximate it by a continuous medium. This will be done by making two assumptions. The first is that Eq. (13) can be converted into a differential equation by setting

$$\Delta I(z,\Omega) = \frac{\Delta I(z,\Omega)}{\Delta s} L \approx \frac{\partial I(z,\Omega)}{\partial s} L = \cos\theta \frac{\partial I(z,\Omega)}{\partial z} L = -\cos\theta \frac{\partial I(\tau,\Omega)}{\partial \tau} EL, \tag{24}$$

where τ is the optical depth as usually defined,

$$\tau = \int_z^\infty E\,\mathrm{d}z'. \tag{25}$$

The second assumes that to a sufficient approximation the discontinuous function $T(s) = (1 - EL)^N$, Eq. (15), can be replaced by the continuous function $T(s) = C\exp(-KEs)$, where s now becomes a continuous variable. The constant C is found by requiring that the irradiance between $s = NL$ and $s = (N+1)L$ in the discontinuous medium, $I_0(1-EL)^N$, be equal to the average irradiance between these two distances in the quasi-continuous medium, $(I_0 C/L)\int_{NL}^{(N+1)L} \exp(-KEs)\,\mathrm{d}s$. This gives $C = K$, so that the transmissivity in the quasi-continuous medium now becomes

$$T(s) = K\exp(-KEs). \tag{26}$$

The quasi-continuous function, Eq. (26), is compared with the discontinuous stair function, Eq. (15), and the function of a continuum, Eq. (14), in Fig. 1.

Hence, in Eq. (13), $T(z/\mu_0) = K\exp(-K\tau/\mu_0)$. Putting $w = S/E$, and dividing by EL, this equation becomes

$$-\cos\theta \frac{\partial I(z,\Omega)}{\partial \tau} = -I(\tau,\Omega) + \frac{w}{4\pi}\int_{4\pi} I(\tau,\Omega')\,\mathrm{d}\Omega' + \frac{w}{4\pi} JK\exp(-K\tau/\mu_0). \tag{27}$$

This expression has the usual form of the radiative transfer equation, except for the factors K in the last term.

The solution for the reflectance using the two-stream approximation is straightforward and identical to that in the author's previous publications (Hapke, 1981, 1993), which should be consulted for details that will not be repeated here. This procedure gives for the bidirectional reflectance

$$r(i,e,g) = K\frac{w}{4\pi}\frac{\mu_0}{\mu_0+\mu} H(\mu_0)H(\mu), \tag{28}$$

where

$$H(x) = \frac{1 + 2x/K}{1 + 2\gamma x/K}, \tag{29}$$

$\gamma = \sqrt{1-w}$, and for a medium of equant particles $K = -\ln(1 - 1.209\phi^{2/3})/1.209\phi^{2/3}$.

The directional-hemispherical reflectance, or plane albedo, is found in a similar manner,

$$r_\mathrm{h}(i) = 1 - \gamma H(\mu_0), \tag{30}$$

where the H-function is defined in (29).

Equation (28) can be readily extended to include a first-order correction for nonisotropic scattering,

$$r(i,e,g) = K\frac{w}{4\pi}\frac{\mu_0}{\mu_0+\mu}\big[p(g) + H(\mu_0)H(\mu) - 1\big]. \tag{31}$$

Corrections for macroscopic roughness and the opposition effect may also be incorporated following Hapke (1984, 1986, 1993, 2002). In most models of the opposition effect the angular width of the peak is predicted to depend on the porosity, which is the subject of this paper. However, several recent experimental papers (Nelson et al., 2002; Piatek et al., 2004; Hapke et al., 2006; Shepard and Helfenstein, 2007) have found either little porosity-dependence or a different one than predicted, so that at the present time it is not clear how to interpret the height and width of the opposition peak in a close packed medium.

Equation (28) is plotted for several angles and single scattering albedos in Figs. 3–5 to illustrate the effects of porosity on the bidirectional reflectance. Note that increasing the filling factor (decreasing the porosity) increases the reflectance, as found experimentally, for all but the highest albedos. The decrease in reflectance when the albedo is close to one is caused by the decreased contribution of multiply scattered light, as predicted by Peltoniemi and Lumme (1992). The shape of the photometric function does not change appreciably, except at high albedos and small angles of incidence (Fig. 5a).

Equations (28) and (31) predict that the reflectance becomes infinite when $EL = 1$, but before that can happen coherent effects become important, which changes the effective optical properties of the particles, so that this model becomes invalid. Hence, these expressions do not apply to solid rocks, nor to extremely compacted pressed powders.

3. Comparison with experiment

Unfortunately, I was unable to discoverer any papers in which the single scattering albedo, reflectance and porosity were all measured independently. Hence, quantitative comparisons of the predictions of this model with experiments are not possible. However, several papers have been published in which reflectances at different degrees of compaction were measured,

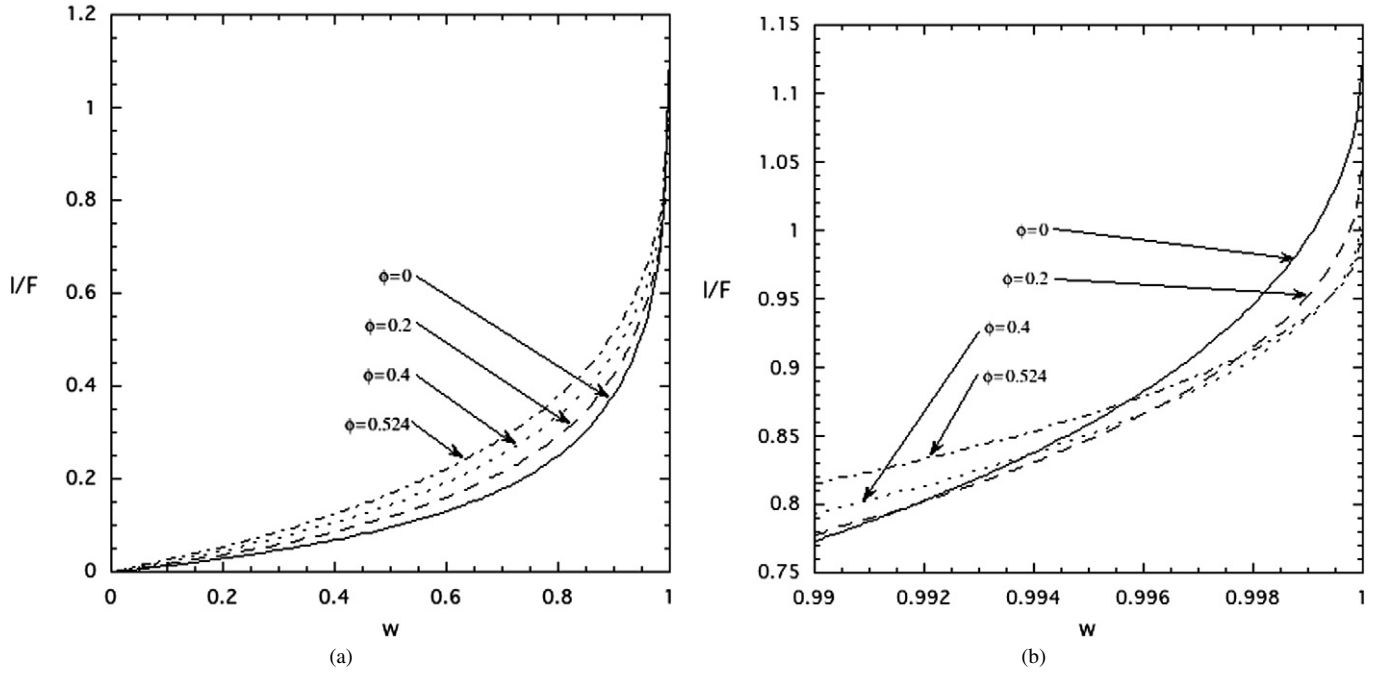

Fig. 3. Radiance factor I/F (reflectance relative to a diffuse surface) at $i = e = g = 0$ (Eq. (28)) vs single scattering albedo w for several different values of the filling factor ϕ. The opposition effect is neglected. Note that the reflectance generally increases with ϕ. (a) Entire range of w; (b) enlarged portion of (a) near $w = 1.00$, illustrating reversal of this trend.

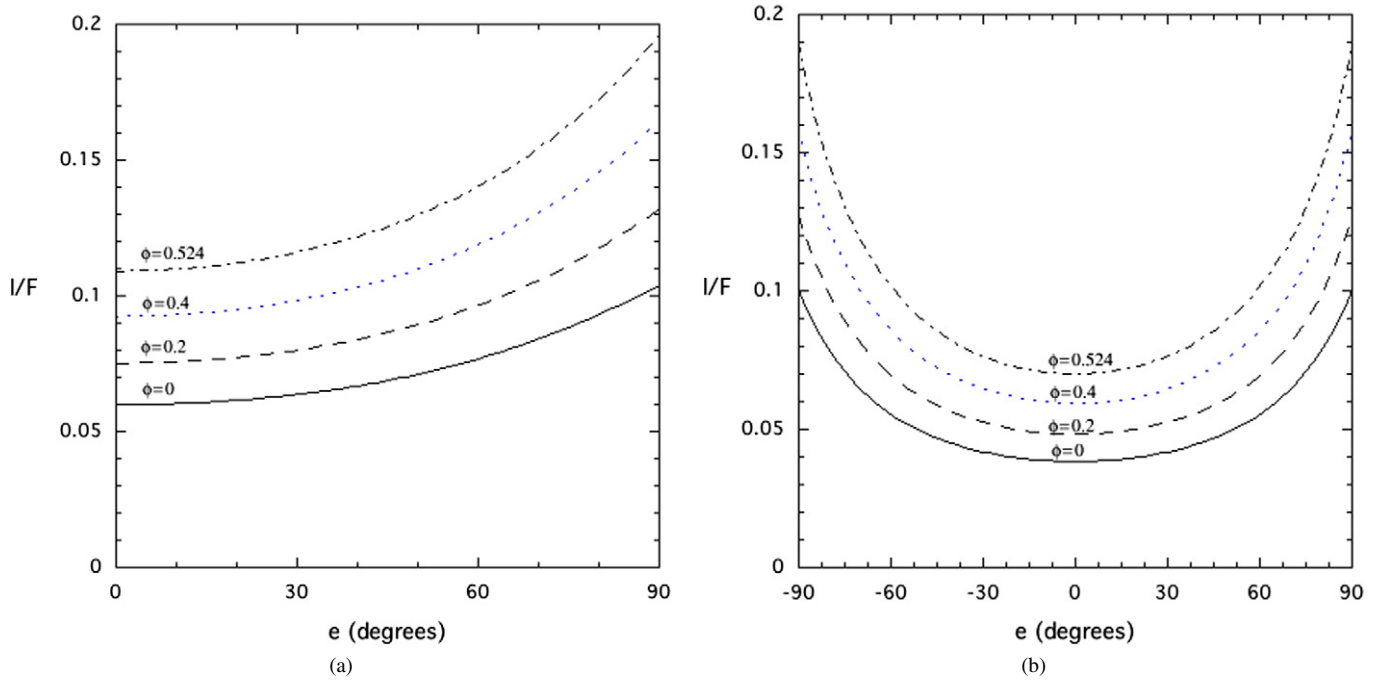

Fig. 4. Radiance factor I/F of a medium with $w = 0.36$ vs viewing angle e for several values of ϕ. (a) $i = 0$; (b) $i = 60°$.

so that qualitative comparisons are possible. These measurements are summarized in Table 1 and Fig. 6. It should be noted that several of the media consist of particles of the order of the wavelength or smaller, and the filling factor for one exceeded the critical value for interference, so that the model is only marginally applicable to those. The main results of these papers may be summarized as follows.

First, increasing the filling factor invariably increases the reflectance. This is consistent with the model, which predicts that only for media of particles with single scattering albedos extremely close to one will an increased filling factor result in a decreased reflectance. Second, Fig. 6 shows that the amount of increase of reflectance with filling factor decreases as reflectance increases, as predicted. Third, the outlier point in

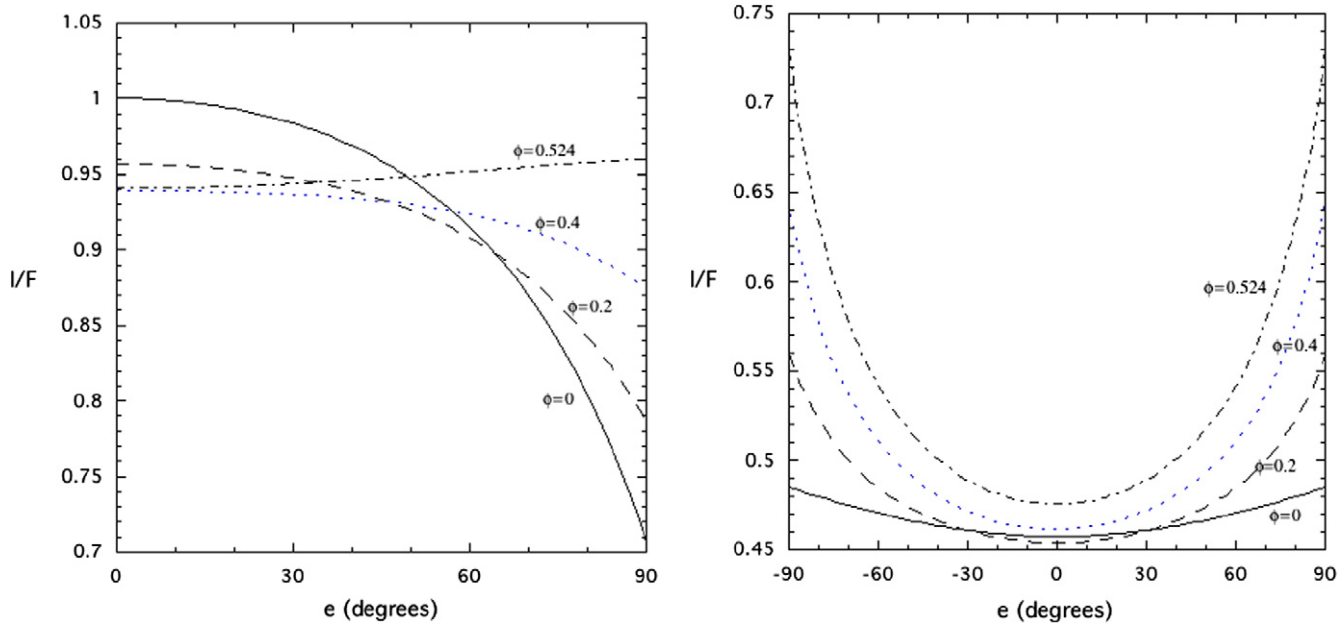

Fig. 5. Radiance factor I/F of a medium with $w = 0.9991$ vs viewing angle e for several values of ϕ. (a) $i = 0$; (b) $i = 60°$.

Table 1
Sample properties

Composition	D (μm)	λ (nm)	Packed		Loose		Reference
			ϕ	I/F[a]	ϕ	I/F[a]	
Co-glass	<37	353	?	0.48	?	0.47	Hapke and Wells (1981)
		448		0.36		0.29	
		554		0.09		0.06	
		690		0.15		0.11	
		820		0.72		0.68	
Blackbird clay	<1	450	0.33	0.09	0.16	0.06	Shepard and Helfenstein (2007)
		550		0.17		0.12	
		700		0.28		0.23	
Chromium oxide	~1	450	0.29	0.09	0.16	0.06	
		700		0.32		0.22	
Al_2O_3	~1	633	0.33	1.11	0.28	1.06	Kaasalainen (2003)
Olivine basalt	75–250	633	0.81?	0.48	0.56?	0.23	Naranen et al. (2004)
Diabase	<74	Broad	0.42	0.24	0.34	0.21	Capaccioni et al. (1990)
Peridotite	<74	Broad	0.41	0.29	0.25	0.24	

[a] For the cobalt glass, $i = 0$, $e = 30$, $g = 30$; for the blackbird clay, chromium oxide, diabase and peridotite, $i = 0$, $e = 20$, $g = 20$; for the Al_2O and olivine basalt, $i = 0$, $e = 0$, $g = 0$ (all angles in degrees).

Fig. 6 corresponds to a sample of basalt that had been subjected to extreme pressure, and shows an enhancement greater than a factor of 2. Figs. 3–5 show that increases of this magnitude are possible.

Another observation that is consistent with the results of this paper is apparent in photographs taken by the Apollo astronauts during their excursions on the lunar surface. Wherever the astronauts walked, the surface is seen to be darker. This lunar disturbance effect was discussed by Hapke (1972), who attributed it to increased shadows cast by clumps of soil particles thrown out by the boots of the astronauts as they moved about the surface. However, the bottoms of the footprints, where the regolith had been compressed, are distinctly brighter than the undisturbed soil.

4. Discussion

The reflectance functions of Hapke (1981, 1993) have been modified to include effects of porosity. The new expressions have the same form as the original ones, with the addition of the porosity factor K (Eq. (16)), and degenerate into the old form when $\phi \ll 1$. The new model exhibits qualitative agreement with existing observations. Porosity dependence arises because the extinction coefficient in the transmissivity of a particulate medium is larger than in an equivalent continuous medium. As the filling factor increases the medium becomes more opaque to light that passes between the particles. The reflectance is proportionately more dominated by the brighter uppermost monolayers where the light can escape more readily, which increases

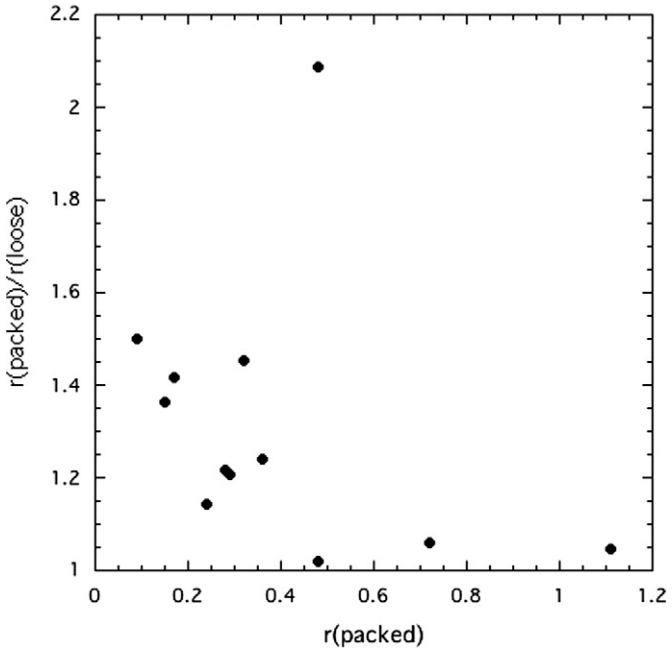

Fig. 6. The ratios of the reflectances of powders in packed form to those of the powders in loose packing plotted against the reflectances of the packed powders, from Table 1.

the reflectance. The angular dependence also changes, although this change is minor except for very high albedos. Eventually, at very high filling factors the particles are squeezed so closely together that coherent interactions between particles become important. When that happens chains and clumps of particles begin to behave like larger single particles, the grains surfaces reflect light less effectively, and the scattering per particle decreases from when the particles are separated. Hence, as the filling factor increases the reflectance of the medium first increases, then goes through a maximum and decreases.

In media of particles comparable to the wavelength in size, such as clays in visible light and lunar regolith in the thermal infrared, coherent effects are important at virtually all filling factors. However, there is evidence (Hapke, 1993; Piatek et al., 2004) that clumps of particles behave as the fundamental scatterers in such media. In that case the equations of this paper would apply to the clumps rather than the individual particles.

At present, coherent interactions in densely packed media can only be treated by exact numerical solution of Maxwell's equations for systems consisting of a few particles (Mishchenko et al., 2007; Petrova et al., 2007), which is totally impractical for realistic regoliths. Interestingly, when such exact solutions are carried out by computer the opposition effect appears naturally. By contrast, it must be added *ad hoc* to our present approximate regolith scattering models. Future research may allow a similar treatment of other coherent effects in densely packed media by semi-empirical correction factors.

One of the objectives of planetary photometry is to be able to invert the measured data to determine properties of the planetary regolith that is reflecting the sunlight. One of the photometric quantities that had been considered fairly robust during such inversions is the single scattering albedo w. However, a change in reflectance caused by porosity-dependence can easily be mistaken for a change in w, as found by Shepard and Helfenstein (2007). Hence, unless limits can be put on the porosity photometric inversions should be interpreted with care. On the other hand, further investigation may lead to tools that allow the remote determination of regolith porosity.

Acknowledgments

I thank Paul Lucey and Paul Helfenstein for constructive suggestions. This research is supported by grant NNG05GG87G from the Planetary Geology and Geophysics Program of the National Aeronautics and Space Administration.

References

Blevin, W., Brown, W., 1961. Effect of particle separation on the reflectance of semi-infinite diffusers. J. Opt. Soc. Am. 51, 129–134.

Capaccioni, F., Cerroni, P., Barucci, M., Fulchignoni, M., 1990. Phase curves of meteorites and terrestrial rocks: Laboratory measurements and applications to asteroids. Icarus 83, 325–348.

Gobel, G., Kuhn, J., Fricke, J., 1995. Dependent scattering effects in latex-sphere suspensions and scattering powders. Waves Random Media 5, 413–426.

Hapke, B., 1972. The lunar disturbance effect. Moon 3, 456–460.

Hapke, B., 1981. Bidirectional reflectance spectroscopy. 1. Theory. J. Geophys. Res. 86, 3039–3054.

Hapke, B., 1984. Bidirectional reflectance spectroscopy. 3. Correction for macroscopic roughness. Icarus 59, 41–59.

Hapke, B., 1986. Bidirectional reflectance spectroscopy. 4. The extinction coefficient and the opposition effect. Icarus 67, 264–280.

Hapke, B., 1993. Theory of Reflectance and Emittance Spectroscopy. Cambridge Univ. Press, Cambridge, UK.

Hapke, B., 1999. Scattering and diffraction of light by particles in planetary regoliths. J. Quant. Spectrosc. Radiat. Trans. 61, 565–581.

Hapke, B., 2002. Bidirectional reflectance spectroscopy. 5. The coherent backscatter opposition effect and anisotropic scattering. Icarus 157, 523–534.

Hapke, B., Wells, E., 1981. Bidirectional reflectance spectroscopy. 2. Experiments and observations. J. Geophys. Res. 86, 3055–3060.

Hapke, B., Nelson, R., Smythe, W., Mannatt, K., 2006. Validity of regolith reflectance models based on the radiative transfer equation and coherent backscatter theory. Bull. Am. Astron. Soc. 38, 605.

Heiken, G., Vaniman, D., French, B., 1991. Lunar Sourcebook. Cambridge Univ. Press, New York.

Ishimaru, A., Kuga, Y., 1982. Attenuation of a coherent field in a dense distribution of particles. J. Opt. Soc. Am. 72, 1317–1320.

Kaasalainen, S., 2003. Laboratory photometry of planetary regolith analogs. I. Effects of grain and packing properties on opposition effect. Astron. Astrophys. 409, 765–769.

Lumme, K., Bowell, E., 1981. Radiative transfer in the surfaces of atmosphereless bodies. 1. Theory. Astron. J. 86, 1694–1704.

Mishchenko, M., Macke, A., 1997. Asymmetry parameters of the phase function for isolated and densely packed spherical particles with multiple internal inclusions in the geometric optics limit. J. Quant. Spectrosc. Radiat. Trans. 57, 767–794.

Mishchenko, M., Dlugach, J., Yanoviskij, E., Zakharova, N., 1999. Bidirectional reflectance of flat, optically thick particulate layers: An efficient radiative transfer solution and applications to snow and soil surfaces. J. Quant. Spectrosc. Radiat. Trans. 63, 409–432.

Mishchenko, M., Liu, L., Mackowski, D., Cairns, B., Videen, G., 2007. Multiple scattering by random particulate media: Exact 3D results. Opt. Express 15, 2822–2836.

Naranen, J., Kaasalainen, S., Peltoniemi, J., Heikkila, S., Granvik, M., Saarinen, V., 2004. Laboratory photometry of planetary regolith analogs. II. Surface roughness and extremes of packing density. Astron. Astrophys. 426, 1103–1109.

Nelson, R., Smythe, W., Hapke, B., Hale, A., 2002. Low phase angle laboratory studies of the opposition effect: Search for wavelength dependence. Planet. Space Sci. 50, 849–856.

Peltoniemi, J., Lumme, K., 1992. Light scattering by closely packed particulate media. J. Opt. Soc. Am. A 9, 1320–1326.

Petrova, E., Tishkovets, V., Jockers, K., 2007. Modeling of opposition effects with ensembles of clusters: Interplay of various scattering mechanisms. Icarus 188, 233–245.

Piatek, J., Hapke, B., Nelson, R., Smythe, W., Hale, A., 2004. Scattering properties of planetary regolith analogs. Icarus 171, 531–545.

Shepard, M., Helfenstein, P., 2007. A test of the Hapke photometric model. J. Geophys. Res. 112, doi:10.1029/2005JE002625. E03001.

Shkuratov, Y., Starukhina, L., Hoffmann, H., Arnold, G., 1999. A model of spectral albedo of particulate surfaces: Implications for optical properties of the Moon. Icarus 137, 235–246.